Theoretical and Experimental Studies of Enflurane. Infrared Spectra in Solution, in Low-Temperature Argon Matrix and Blue Shifts Resulting from Dimerization

ARTICLE *in* THE JOURNAL OF PHYSICAL CHEMISTRY B · NOVEMBER 2007

Impact Factor: 3.3 · DOI: 10.1021/jp073772r · Source: PubMed

Theoretical and Experimental Studies of Enflurane. Infrared Spectra in Solution, in Low-Temperature Argon Matrix and Blue Shifts Resulting from Dimerization

Danuta Michalska,[†] Dariusz C. Bieńko,[†] Bogusława Czarnik-Matusewicz,*[,‡] Maria Wierzejewska,[‡] Camille Sandorfy,[§] and Thérèse Zeegers-Huyskens*[,||]

Faculty of Chemistry, Wrocław University of Technology, Wybrzeże Wyspiańskiego, 50-370 Wrocław, Poland, Faculty of Chemistry, University of Wrocław, F. Joliot-Curie 14, 50-383 Wrocław, Poland, Département de Chimie, Université de Montréal, Montréal, Québec, Canada H3C 347, and Department of Chemistry, University of Leuven, 200F Celestijnenlaan, 3001 Leuven, Belgium

Received: May 16, 2007; In Final Form: July 20, 2007

Theoretical studies are performed on enflurane ($CHFCl-CF_2-O-CHF_2$) to investigate the conformational properties and vibrational spectra. Calculations are carried out at the B3LYP/6-31G(d) level along with a natural bond orbital (NBO) analysis. Experimental infrared spectra are investigated in carbon tetrachloride solution at room temperature and in argon matrix at 12 K. In agreement with previously reported data (Pfeiffer, A.; Mack, H.-G.; Oberhammer, H. *J. Am. Chem. Soc*. **1998**, *120*, 6384), it is shown that the four most stable conformers possess a trans configuration of the C−C−O−C skeleton and a gauche orientation of the CHF_2 group (with respect to the central C−O bond). These conformations are favored by electrostatic interaction between the H atom of the CHF_2 group and the F atoms of the central CF_2 group. Hyperconjugation effects from the O lone pairs to the antibonding orbitals of the neighboring C−H and C−F bonds also contribute to the stability of the four conformers. The vibrational frequencies, infrared intensities, and potential energy distributions are calculated at the same level of theory for the most stable conformers. On the basis of the theoretical results, these conformers are identified in an argon matrix. The influence of the concentration on the ν(CH) vibrations suggests the formations of higher aggregates in solution. Theoretical calculations are carried out on the enflurane dimer. The results show that the dimer is formed between two enflurane conformers having the largest stability. The dimer has an asymmetric cyclic structure, the two enflurane molecules being held together by two nonequivalent C−H···F hydrogen bonds, the C−H bond of the CHFCl group acting as a proton donor, and one of the F atoms of the CHF_2 groups acting as a proton acceptor. The theory predicts a contraction of 0.0014−0.0025 Å of the two CH bonds involved in the interaction along with a blue shift of 30−38 cm^{-1} of the corresponding ν(C−H) bands, in good agreement with the blue shifts of 35−39 cm^{-1} observed in an argon matrix.

1. Introduction

Methyl or ethyl ethers and their halogenated derivatives have been known for many years to possess anesthetic properties. It is a fact that all general anesthetics act by perturbing intermolecular interactions such as van der Waals interactions or hydrogen bonds without breaking or forming covalent bonds.[1] More specifically, fluorinated ethers such as isoflurane ($CF_3-CHCl-O-CHF_2$)[2] and desflurane ($CF_3-CHF-O-CHF_2$)[3] are known to be very good anesthetics. Enflurane ($CHFCl-CF_2-O-CHF_2$) has been released as a highly volatile narcotic gas. The properties of these anesthetics are related to the presence of CH groups that can act as proton donors, while the electron-withdrawing F or Cl atoms tend to make the hydrogen atoms more acidic than in simple ethers. The action of anesthetics depends on specific binding with proteins, and, therefore, a detailed understanding of such interactions requires the knowledge of conformational and structural properties of these compounds. These properties have been discussed for desflurane[2] and isoflurane.[3] For a gas-phase structural study, enflurane is the most complicated among the widely used inhalation anesthetics because of the large number of possible conformers. The conformations of enflurane have been investigated by various experimental techniques such as the NMR spectroscopy,[4a] gas electron diffraction,[4b] and vibrational circular dichroism (VCD).[4c] Theoretical studies were carried out using both the ab initio and the density functional methods to calculate the energies of the different conformers.[4b,c]

Anomeric effects are known to stabilize the structure of many organic compounds but have not been discussed for enflurane, so far. In the first part of the present Article, we will apply natural bond orbital (NBO) analysis to discuss the hyperconjugation in the most stable conformers of enflurane. The second part of our work deals with the experimental infrared spectrum (3200−700 cm^{-1}) recorded in solution at room temperature and in low-temperature argon matrices. The vibrational modes are assigned on the basis of the calculated potential energy distribution (PED). Up to now, the VCD spectrum of enflurane has been investigated between 1400 and 1000 cm^{-1} in carbon disulfide solution,[4c] but so far the vibrational frequencies have not been assigned. In the third part of this work, a theoretical model for the interaction between two enflurane molecules is

* Corresponding authors. E-mail: bc@wchuwr.pl (B.C.-M.); therese.zeegers@chem.kuleuven.be (T.Z.-H.).
[†] Wrocław University of Technology.
[‡] University of Wrocław.
[§] Université de Montréal (deceased on June 6, 2006).
[||] University of Leuven.

10.1021/jp073772r CCC: $37.00
Published on Web 10/03/2007

presented. The results of a NBO analysis and the vibrational frequencies predicted for the dimer are discussed. The last section deals with the infrared spectra of neat enflurane along with the infrared spectra of enflurane in an argon matrix. The theoretical predictions are compared with the experimental features.

2. Methods

2.1. Experimental. The infrared spectra of neat enflurane and of enflurane in carbon tetrachloride at concentrations ranging from 0.01 to 5.20 mol dm^{-3} were measured between 4000 and 400 cm^{-1}. KBr and quartz cells having thickness between 24 μm and 20 mm were used in the experiments. The spectra were recorded in transmission mode with a resolution of 1 cm^{-1} on a Nicolet Magna 860 FTIR spectrometer equipped with a Globar source, KBr beamsplitter, and DTGS detector. Data processing (removing of fluctuating baseline and noise, evaluation of parameters of the asymmetric ν(CH) bands, resolution of overlapping bands) was performed by the Grams 32/AI program package (Galactic Inc. Corp.).

The matrix isolation spectra were taken at enflurane/Ar matrix ratios equal to 1/600, 1/1500, and 1/3000. The gas mixtures were condensed on a gold-plated copper mirror maintained at 12 K by means of a closed cycle helium refrigerator, Air Products, Displex 202A. The infrared spectra between 4000 and 500 cm^{-1} were recorded in reflection mode on a Bruker 113v FTIR spectrometer equipped with a liquid nitrogen cooled MCT detector. The resolution was 0.5 cm^{-1}.

The products were purchased from Fluka (enflurane) and from Applichem GmbH (carbon tetrachloride).

2.2. Theoretical. Full geometry optimizations of the four conformers of isolated enflurane were performed by the density functional three-parameter model (B3LYP)5 using the 6-31G(d) basis set, and by the MP2 method with the 6-311G(d) basis set. Several initial structures of dimers were considered. They were constructed from the A−A, A−B, A−C, and A−D molecules oriented in the "head-to-tail" fashion. Both the A−C and the A−D hypothetical heterodimers are unstable due to a repulsive interaction between the C−FF group in A component and the C−Cl group in C or D component. Full geometry optimization of both the A−A and the A−B initial structures leads to the same dimer described as $A_1\cdots A_2$. However, it should be noted that the conformation of the A_1 subunit is very similar to that of the A monomer, while the conformation of the A_2 subunit is something between the structures of A and B monomers. Geometry optimization of the $A_1\cdots A_2$ dimer was followed by the calculations of the vibrational frequencies and infrared intensities performed at the B3LYP/6-31G(d) level of theory. It is worth mentioning that the VCD spectrum of enflurane predicted at the same level of theory showed better agreement with the experimental VCD spectrum than that obtained in the B3PW91/6-311G(2d) calculations.[4c] The normal coordinate analyses have been carried out for the investigated monomers and dimer according to the procedure described earlier.[6] The nonredundant sets of 30 internal coordinates for each monomer and of 66 internal coordinates for dimer were defined. The calculated potential energy distributions (PEDs) have enabled us to make comparison between the frequencies of the corresponding normal modes in the four monomers, and in the dimer of enflurane. Charges on individual atoms, orbital occupancies, and hyperconjugative energies were obtained by a NBO analysis.[7] The binding energy of dimer (ΔE) was calculated as the difference between the total energy of the dimer and the energies of the monomers calculated in the respective monomer basis sets. ΔE was corrected for basis set superposition error (BSSE) using the counterpoise (CP) method of Boys and Bernardi,[8a] as implemented in the Gaussian 03 package.[8b] The Gaussian set of programs[8c] was used for all of the calculations reported in this work.

3. Results and Discussion

3.1. Conformation of Enflurane. The question of predominant conformation of enflurane has been addressed in previous works[4b,c] and will be briefly summarized here, because the conformational equilibrium is the starting point of the present research. Enflurane possesses in principle 27 different conformations.[4b] The lowest energy conformers are shown in Figure 1. They are all characterized by a C1−C2−O3−C4 fragment having the trans conformation. The dihedral C1−C2−O3−C4 angle does not greatly differ from 180°. Structures A, B, and C differ by the rotational orientation of the CHFCl group, with Cl (A), F6 (B), and H5 (C and D) trans to the C2−O3 bond. The four conformers are characterized by a gauche orientation of the C2−O3−C4−H12 group where the C4−H12 bond is in trans position with respect to the lone pair orbital of the O3 atom. The C2−O3−C4−H12 dihedral angle is about 18° for the A, B, and C conformers. For the D conformer, this angle is smaller (7°). Dihedral angles for A, B, C, and D and distances between the bonded atoms for A have been reported in earlier works.[4b,c] Relevant distances and angles for the A, B, C, and D conformers are indicated in Table 1. Our results show that the bond lengths are very similar, except the C−F lengths. This will be discussed more in detail at the end of this section.

The relative energies of the conformers along with their conformational composition calculated at different levels of theory (MP2/6-311G(2d),[4b] B3PW91/6-311G(2d)[4b,c]) are indicated in Table 2. Our calculations carried out at the MP2/6-311G(d) level are in good agreement with previous results showing that the A and B conformers are slightly more stable than the C and D ones. The gas electron diffraction experimental data have shown that the A conformer is the predominant form, but the C and D conformers could not be distinguished. The difference in energy is small so that all four conformers are expected to be present at 298 K. The dipole moments of the four conformers are equal to 0.76, 0.72, 2.31, and 2.33 D, respectively.

Now, we want to discuss in more detail the conformation of the $F_2C-O-CHF_2$ fragment of enflurane. It is well known that in $R-O-CX_3$ molecules, anomeric effects resulting from a negative hyperconjugation between the lone pair orbital(s) of the O atom and the σ^* antibonding orbital of the C−X bond in trans position with respect to the lone pair orbital(s) exert a strong influence on the conformational properties of these molecules.[9]

It is interesting to compare the hyperconjugation effect in enflurane and in fluorinated ethers. The most stable conformation of CH_3-O-CH_2F[10] is characterized by the C−F bond being in trans position with respect to the O lone pair orbital. A recent theoretical investigation has shown that in all of the fluorinated dimethyl ethers, in the symmetric as well as in the asymmetric derivatives, the most stable conformation corresponds to a gauche orientation of the C−F bond(s), with respect to the O lone pairs, the only exception being $CH_3-O-CHF_2$ where the C−H bond of the CHF_2 group is in trans position with respect to the O lone pair.[11] The hyperconjugative energies from the O lone pairs to the σ^*(C−F) orbital(s) are rather large. The CH_3-O-CH_2F molecule is an illustrative example of the influence of hyperconjugation on the conformational stability. In the most

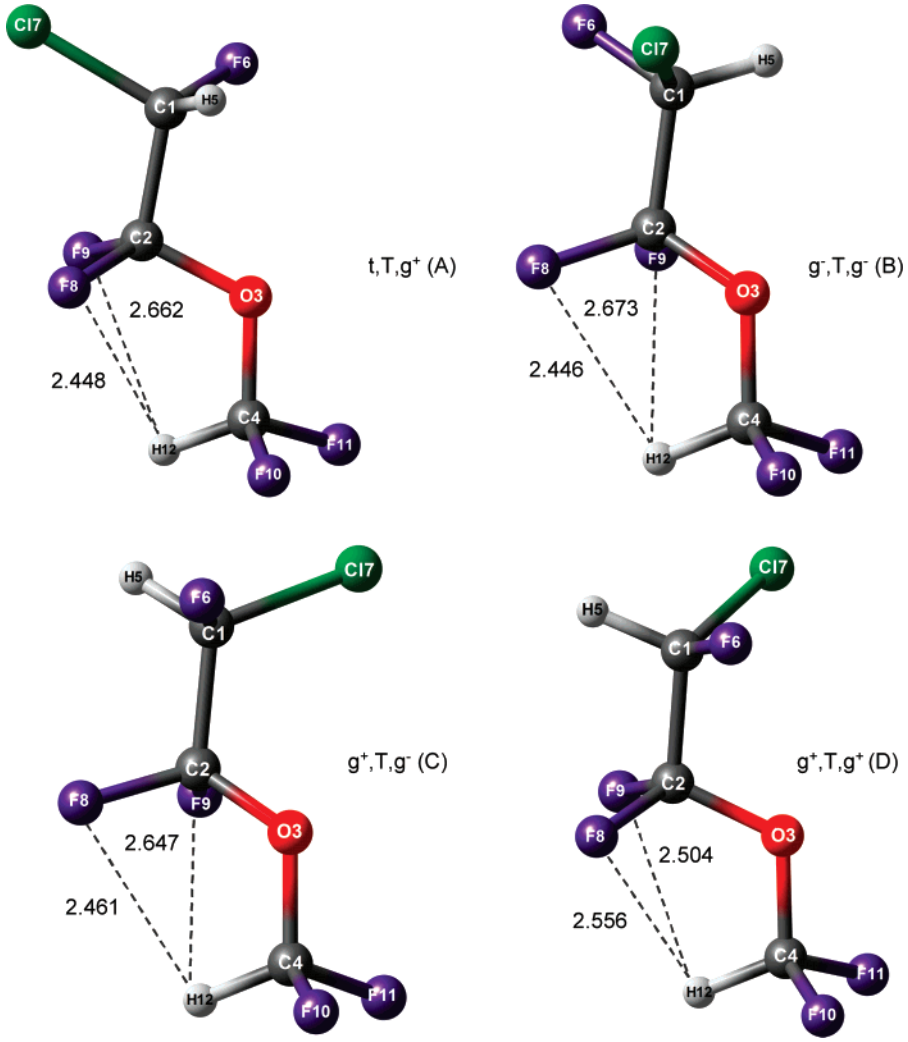

Figure 1. The four most stable conformations of enflurane: t,T,g^+ (A), g^-,T,g^- (B), g^+,T,g^- (C), and g^+,T,g^+ (D). The first letter characterizes the orientation of the Cl atom relative to the central C2−O3 bond, the second letter (capital letter) describes the structure of the C2−C2−O3−C4 skeleton, and the third letter specifies the orientation of H12 relative to the central C2−O3 bond (dihedral angle C2−O3−C4−H12).

TABLE 1: B3LYP/6-31G(d) Optimized Geometries of the A, B, C, and D Conformers of Enflurane (Distances in Å, Angles in deg)[a]

	A	B	C	D
C1−H5[b]	1.0910	1.0912	1.0918	1.0918
C1−F6	1.357	1.358	1.357	1.357
C1−Cl7	1.789	1.788	1.787	1.788
C1−C2	1.538	1.537	1.536	1.536
C2−F8	1.359	1.356	1.366	1.365
C2−F9	1.356	1.362	1.359	1.361
C2−O3	1.373	1.370	1.363	1.363
O3−C4	1.399	1.399	1.399	1.399
C4−H12[a]	1.0912	1.0912	1.092	1.091
C4−F10	1.348	1.342	1.342	1.346
C4−F11	1.342	1.348	1.347	1.344
C1−C2−O3	107.3	109.0	110.9	110.9
Cl−C1−C2−O3	−179.1	−64.4	61.9	62.3
C1−C2−O3−C4	−177.5	−176.4	178.6	177.0
C2−O3−C4−H12	17.8	−18.6	−18.1	7.4
H5−C1−C2−O3	−60.0	55.1	−179.3	−178.9

[a] The C2−O3−C4, H−C−F, H−C−Cl, and F−C−F angles are very similar in the four conformers. [b] The C−H distances are given with 4 digits as usual for blue-shifted hydrogen bonds.

stable conformer, where the C−F bond is in trans position to the O lone pair, the nO → σ^*(C−F) hyperconjugative energy is 19.4 kcal mol^{-1}. Interestingly, in the less stable conformer, where both of the C−H bonds are in trans position to the O lone pairs, there are hyperconjugation effects from the two oxygen lone pairs not only to the σ^*(C−F) bond but also to the σ^*(C−H) bonds. Calculations show that, in this case, the hyperconjugative energy of the first O lone pair, nO(1) → σ^*(C−F), is equal to 5.4 kcal mol^{-1}, while that of the second O lone pair, nO(2) → σ^*(C−H), is equal to 7.1 kcal mol^{-1}.[11]

TABLE 2: Relative Energies (ΔE in kcal mol^{-1}) of the A, B, C, and D Conformers of Enflurane and Conformational Composition (in Parentheses) Calculated at Different Levels of Theory

conformer	MP2/6-311G(2d)[a]	B3PW91/6-311G(2d)		B3LYP/6-31G(d)[b]	MP2/6-311G(d)[c]
A	0.04	0[a]	0.34[b]	0	0.07
	(27)	(29)	(19)	(30)	(31)
B	0	0.03	0	0.16	0
	(29)	(27)	(34)	(23)	(35)
C	0.16	0.15	0.44	0.41	0.42
	(44)[d]	(44) [d]	(16)	(15)	(17)
D	0.17	0.16	0.18	0.18	0.44
	(44)[d]	(44) [d]	(25)	(22)	(17)

[a] Reference 4b. [b] Reference 4c. [c] This work. [d] Sum of the C and D conformers.

TABLE 3: Relevant NBO Data for the C−H and C−F Bonds of the A, B, C, and D Conformers of Enflurane (Hyperconjugation Energies (kcal mol^{-1}) and Occupation of σ^* Orbitals (e))

donor[a]/acceptor	hyperconjugation energies A	B	C	D
nO(1) → σ^*(C4−H12)	3.6	3.6	3.7	3.9
nO(2) → σ^*(C2−F8)	14.5	14.3	15.5	15.0
nO(2) → σ^*(C2−F9)	13.9	15.0	15.0	15.7
nO(2) → σ^*(C4−F10)	13.5	6.0	6.2	11.9
nO(2) → σ^*(C4−F11)	6.2	13.8	13.6	8.5

acceptor non Lewis NBOs	occupation of σ^* orbitals A	B	C	D
σ^*(C1−H5)	0.033	0.033	0.032	0.032
σ^*(C4−H12)	0.045	0.045	0.046	0.045
σ^*(C2−F8)	0.109	0.107	0.116	0.114
σ^*(C2−F9)	0.107	0.112	0.110	0.112
σ^*(C4−F10)	0.091	0.080	0.080	0.088
σ^*(C4−F11)	0.080	0.091	0.091	0.084

[a] nO(1) is the first lone-pair orbital (sp$^{1.5}$ hybridization) on the oxygen atom; nO(2) is the second lone-pair orbital (p_z) on the oxygen atom.

Thus, hyperconjugation energies to the σ^*(C−H) bonds in trans position are by no means negligible.

These results can be compared with the data of enflurane obtained in the present work. It must be noticed that the relative energies of the gauche and trans orientations of the CHF_2 group (H gauche or trans with respect to the central C2−O3 bond) do not markedly differ. According to the ab initio HF calculations, the differences in energy are of the order of magnitude of 1−2 kcal mol^{-1}.[4b] As discussed in ref 4b, it might be expected that in enflurane, the anomeric effect between the oxygen lone pairs and the σ^*(C−F) orbitals of the CHF_2 group stabilizes the conformation for which both fluorine atoms F10 and F11 are gauche with respect to the C2−O3 bond.

However, conjugation energies have not been calculated in ref 4b. According to our results, the hyperconjugative energies in the four A, B, C, and D conformers of enflurane are not negligible. The results reported in Table 3 show that there is a hyperconjugative effect of more than 3 kcal mol^{-1} from the first O lone pair orbital (sp$^{1.5}$ hybridization) to the σ^*(C4−H12) orbital. The hyperconjugative energies from the second O lone pair (pure p-orbital) to the σ^*(C4−F10) and σ^*(C4−F11) orbitals are between 6 and 13.8 kcal mol^{-1}, depending on the orientation of the CHF_2 group. These values are smaller than 19.4 kcal mol^{-1} predicted for the trans orientation of the C−F bond with respect to the O lone pair orbital in CH_3−O−CHF_2.[11] However, these interactions may stabilize the gauche conformers of enflurane (where both fluorine atoms, F10 and F11, are gauche with respect to the C2−O3 bond). Interestingly, hyperconjugative energies from the second O lone pair orbital to the C2−F8 and C2−F9 bonds in trans position to this orbital are larger, that is, take values between 13.9 and 15.7 kcal mol^{-1}.

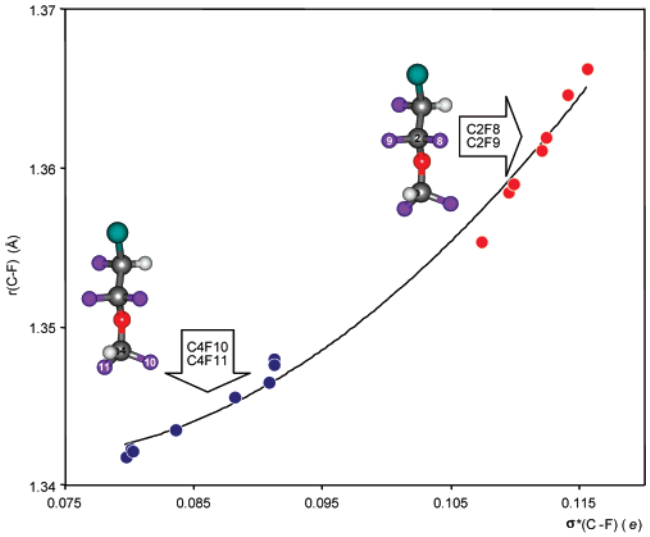

Figure 2. The r(C−F) distance (Å) as a function of σ^*(C−F) (e).

Higher hyperconjugative energies correspond to a larger occupation of the σ^*(C−F) orbitals and larger C−F distances. The smallest C4−F10 distance of 1.342 Å (for B and C) conforms to the smallest occupation of the corresponding σ^* orbital (0.080 e), while the largest C2−F8 distance of 1.366 Å is accompanied by a relatively large occupation of the σ^* orbital (0.116 e). Our results demonstrate that there is a correlation between the C−F distances (including the C2−FF and C4−FF fragments in the four conformers) and the occupation of the corresponding σ^*(C−F) orbitals. The best fit has been found for a second-order polynomial:

$$r(\mathrm{C-F}) = 1.3992 - 1.6342\sigma^*(\mathrm{C-F}) + 11.5870\sigma^*(\mathrm{C-F})^2 \quad (r = 0.9871) \quad (1)$$

which is illustrated in Figure 2.

The conformation of the F_2C−O−CHF_2 fragment of enflurane was explained by steric repulsions between the F8 (F9) and F10 (F11) atoms that apparently override the anomeric effect.[4b] Electrostatic repulsion between the negatively charged F atoms must destabilize the structure as well. On the other hand, an electrostatic attraction between the H12 and the F8 and F9 atoms contributes to stabilization of the structure. Indeed, in the A conformer, the NBO charge on the H12 atom is equal to +0.18 e and the charge on the F8 and F9 atoms is −0.36 e. This explanation is supported by the fact that in all of the conformers, the H12···F8 and H12···F9 distances are relatively short, comprising between 2.446 and 2.673 Å. Analogous justification has been provided to explain the stability of the

TABLE 4: Calculated Frequencies and Infrared Intensities (km mol^{-1}, in Parentheses) in the A, B, C, and D Conformers and PED in the A Conformer of Enflurane

mode	A	B	C	D	PED (A)[a]
Q1	3157 (26)	3158 (26)	3153 (29)	3156 (28)	νC4H12 (100)
Q2	3151 (8)	3148 (9)	3142 (9)	3142 (9)	νC1H5 (100)
Q3	1453 (44)	1456 (40)	1454 (36)	1460 (35)	βH12CO (83)
Q4	1422 (58)	1423 (52)	1424 (56)	1423 (66)	γH12CO (84)
Q5	1408 (47)	1407 (46)	1409 (26)	1409 (14)	βH5CC (47), γH5CC (13), νC1C2 (12)
Q6	1334 (27)	1333 (32)	1336 (64)	1336 (72)	γH5CC (67)
Q7			1322 (167)	1324 (157)	νC2O (30), βH5CC (25), γH5CC (19)
Q7	1301 (124)	1301 (133)			βH5CC (27), ν^{s}C2FF (16), νC1C2 (11)
Q8	1212 (227)	1229 (226)	1206 (390)	1194 (304)	νC2O (58)
Q9	1196 (288)	1193 (271)	1176 (128)	1188 (377)	νC4F11 (59), ν^{as}C2FF (13)
Q10	1158 (17)	1157 (286)	1167 (341)	1166 (210)	νC4F10 (43), ν^{as}C2FF (22)
Q11	1152 (535)	1150 (300)	1149 (111)	1149 (98)	νC4F10 (25), νC2O (16) ν^{as}C2FF (13)
Q12	1137 (81)	1135 (107)	1136 (57)	1138 (48)	νC1F6 (68)
Q13	1071 (296)	1057 (181)	1076 (311)	1075 (315)	νC4O (73)
Q14	897 (5)	890 (44)	915 (24)	916 (2)	ν^{s}C2FF (47), νC1C2 (13)
Q15	806 (83)	817 (102)	827 (114)	827 (115)	νC1C7 (39), γF6CC (16), βCCO (13)
Q16	754 (80)	774 (53)	707 (25)	704 (29)	wC2FF (26), βF6CC (13)

[a] Abbreviations: ν = stretching, ν^{s} and ν^{as} = symmetric and asymmetric stretching of the C2FF group, β = in-plane deformation, γ = out-of-plane deformation, w = wagging vibration.

CHF_2-O-CF_3 conformer, where the distance between the H atom and the nearest F atom of the CF_3 group is short (2.468 Å).[11]

3.2. Theoretical and Experimental Infrared Spectra of Enflurane. In this section, we will discuss the theoretical and experimental spectrum of enflurane in dilute carbon tetrachloride solution and in low-temperature argon matrix. The calculated frequencies and infrared intensities of the four conformers and the potential energy distribution (PED) of A conformer are reported in Table 4. The PEDs for the corresponding normal modes in four conformers are very similar, except for the vibrations predicted between 1300 and 1325 cm^{-1}. The mode Q7 calculated at 1301 cm^{-1} has a predominant βH5CC character for A and B conformers. In the case of C and D conformers, mode Q7 is predicted at 1322 and 1324 cm^{-1}, respectively, and it arises mainly from the νC2O stretching vibration. Thus, it can be anticipated that this region will be sensitive to the conformation.

There are also other vibrations sensitive to the conformation of enflurane. This concerns the νC4F11 vibration (mode Q9) predicted at 1196 cm^{-1} in A, and 1176 cm^{-1} in C, and the ν^{s}C2FF vibration (mode Q14) calculated at 890 cm^{-1} in B, and at 916 cm^{-1} in D. Moreover, the frequency of mode Q16 (arising from the coupled wagging and bending vibrations) is also very sensitive to the conformation of enflurane: it is calculated at 774 cm^{-1} in B, 754 cm^{-1} in A, 707 cm^{-1} in C, and 704 cm^{-1} in D. Our theoretical data indicate that the νC4H12 vibration should be observed at higher frequency and with a larger infrared intensity than the νC1H5 stretching vibration. The difference between the frequencies of the four conformers spans a range of only 5 cm^{-1} for the νC4H12 vibration and of 9 cm^{-1} for the νC1H15 vibration.

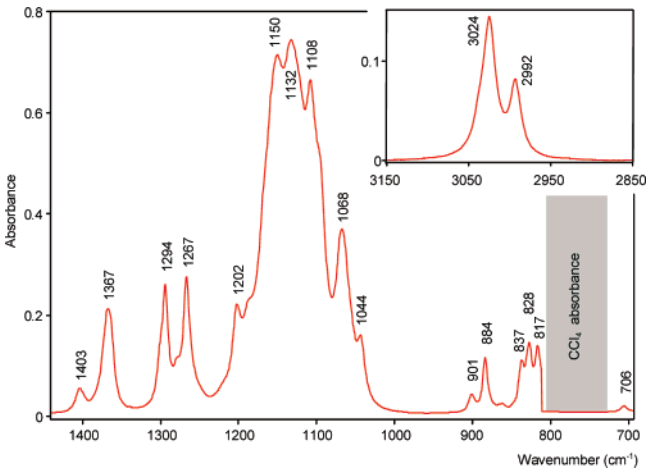

Figure 3. Experimental infrared spectrum (3150−2850 cm^{-1} and 1400−700 cm^{-1}) of enflurane in carbon tetrachloride (c = 0.1 mol dm^{-3}, T = 298 K).

In a next step, we will discuss the experimental infrared spectrum of enflurane in solution and in argon matrices. The infrared spectrum in dilute carbon tetrachloride solution (0.1 mol dm^{-3}) is reproduced in Figure 3. It must be noticed that the infrared spectrum of enflurane in dilute carbon disulfide has been investigated between 1400 and 1000 cm^{-1}.[4c] The wavenumbers of the bands at 1364, 1292, and 1263 cm^{-1} and a broad absorption with several submaxima culminating at 1130

TABLE 5: Experimental Frequencies (3050−700 cm^{-1}) in Dilute Carbon Tetrachloride Solution at 298 K and in Argon Matrix at 12 K

		argon matrix			
mode	CCl4	A	B	C	D
Q1	3024	3025	3029	3019	3021
Q2	2992	3008	3006	2997	2997
Q3	1403	1406	1412	1409	1414
Q4	1367	1374	1374	1374	1374
Q5	n.o.[a]	1359	1359	1362	1364
Q6	n.o.	n.o.	n.o.	n.o.	n.o.
Q7	1294 (C,D) 1267 (A,B)	1266	1266	1296	1298
Q8	1202	1194	1209	1191	1176
Q9	1150	1163	1163	1145	1157
Q10	1132	1135	1135	1141	1138
Q11	n.o.	1127	1123	1120	1120
Q12	1108	1111	1115	1111	1115
Q13	1068	1058	1042	1066	1063
Q14	884 (A,B) 901 (C,D)	890	888	907	907
Q15	817 (A) 828 (B) 837 (C,D)	830	836	847	842
Q16	706 (C,D)[b]	754	767	706	703

[a] Not observed. [b] The vibrational modes of A and B that are predicted around 750 and 770 cm^{-1}, respectively, could not be observed due to the absorption of CCl_4 between 720 and 820 cm^{-1}.

cm^{-1}, reported in ref 4c, are in good agreement with the present data. However, these bands have not been assigned, until now. The assignment of the experimental frequencies observed in solution has been obtained from the theoretical calculations and is presented in Table 5.

In carbon tetrachloride, two absorptions are observed at 3024 and 2992 cm^{-1}, where the band of the higher wavenumber is characterized by a larger intensity than the other band. Fermi resonance between the fundamental νCH vibration and the first overtone of the δCH bending vibrations is often observed. In the present case, this resonance can be ruled out because the energy gap between these two transitions is too large. The in-plane and out-of-plane vibrations of the H12CO groups are indeed observed at 1403 and 1367 cm^{-1}, respectively; therefore, their overtones should appear below 2800 cm^{-1} in the spectrum. Our calculations predict the νC4H12 vibration at higher frequencies than the νC1H5 one. Therefore, the experimental absorptions observed at 3024 and 2992 cm^{-1} are assigned to the νC4H12 and νC1H5 vibrations, respectively. Furthermore, according to the theoretical results, the νC1H5 vibration has much lower infrared intensity than the νC4H12 one. This is in good agreement with the experimental observations. The frequency difference between the conformers is relatively small so that the presence of a mixture of conformers in solution may cause merely a broadening of the experimental νCH absorptions.

Only three modes (Q7, Q14, and Q15) are observed as separated absorptions for different conformers, as shown in Table 5. The first absorption with a maximum at 1294 cm^{-1} is assigned to the C and D conformers, and the second one, located at 1267 cm^{-1}, is attributed to the A and B conformers. This is supported by the VCD spectrum in carbon disulfide showing a negative−positive pair of bands associated with the absorptions at 1292 and 1263 cm^{-1}.[4c] Further, the mode Q14, involving predominantly the ν^sC2FF symmetric stretching vibration, is observed at 884 cm^{-1} in A and B, and at 901 cm^{-1} in C and D. The mode Q15 has a main contribution from the νCCl vibration and is located at 817 cm^{-1} for A, 828 cm^{-1} for B, and 837 cm^{-1} for C and D. From these data, it can be concluded that at least four different conformers are responsible for the detected spectral features.

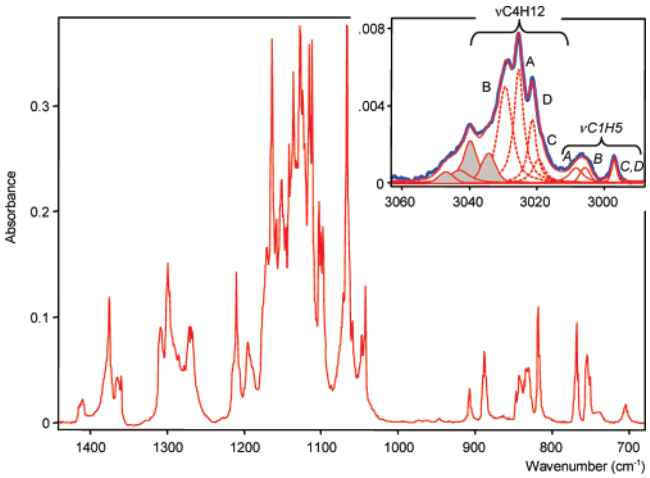

Figure 4. Experimental infrared spectrum (3060−2850 cm^{-1} and 1400−700 cm^{-1}) of enflurane in an argon matrix (ratio enflurane/argon = 1/1500, T = 12 K). Absorptions assigned to the dimer are indicated by the shadowed area.

The infrared spectrum of enflurane in an argon matrix (ratio enflurane/argon equal to 1500) at 12 K is shown in Figure 4. The experimental frequencies along with the assignment of the vibrational modes are summarized in Table 5. As expected, most of the observed frequencies are slightly higher in Ar matrix than in carbon tetrachloride solution.[12]

Special attention will be paid to the spectrum in the 3000 cm^{-1} region. Because the predicted frequencies of the νCH vibrations in the four conformers are rather close, the frequencies of the νC4H12 and νC1H5 vibrations for each conformer were obtained after deconvolution of the spectra. The results of this procedure are shown in Figure 4, and the frequencies are listed in Table 5.

The same frequency (2997 cm^{-1}) has been obtained for C and D conformers, which is in agreement with the theoretical predictions for the Q2 mode. From comparison of the absorbances of the fitted bands with the predicted infrared intensities, the relative concentrations of the conformers have been estimated as: A ≈ 35%; B ≈ 39%; C+D ≈ 26%. This is in good agreement with the gas-phase data reported in Table 2, indicating that A and B are the predominating species. No splitting of the Q4 mode could be observed; there is only one band at 1374 cm^{-1} characteristic of the four conformers. The Q6 mode involving a predominant γH15CC vibration could not be observed, nor in a solution, neither in argon matrix. Most of the other vibrational modes of the conformers could be separately detected in argon. Some of the modes having nearly the same frequency in C and D could be resolved in the spectrum. This is the case of the absorption observed at 1294 cm^{-1} in solution that splits into a doublet (1296/1298 cm^{-1}) in argon, characteristic of the C and D conformers. Such a splitting is supported by the theoretical calculations, which predicted for the Q7 mode a difference of only 2 cm^{-1} between the C and D conformers. The same remark also holds for the band observed at 706 cm^{-1} in solution that splits into two components at 706 (C) and 703 cm^{-1} (D). Further, due to an overlap with the broad absorption culminating at 1150 cm^{-1}, the Q11 mode could not be identified in solution. In argon matrix, the 1127 cm^{-1} absorption is attributed to A, 1123 cm^{-1} to B, while a band at 1120 cm^{-1} is assigned to C and D conformers. The relative intensities of these bands indicate that A and B are largely

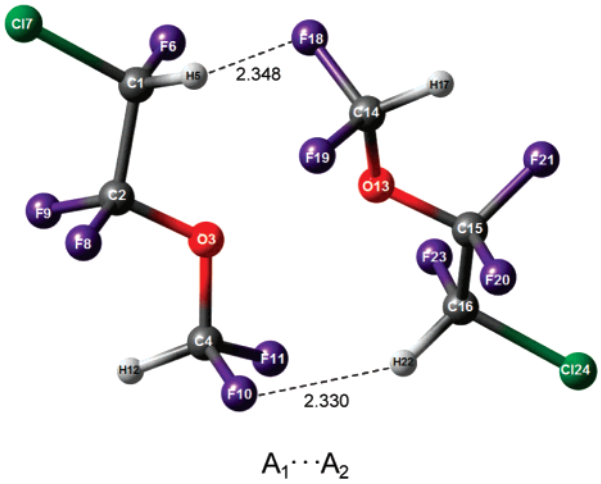

Figure 5. B3LYP/6-31G(d) optimized geometry of the $A_1\cdots A_2$ dimer.

predominating in argon. The same remark also holds for the absorption at 1135 cm^{-1} attributed to both A and B conformers.

It is important to note that the νC4H12 absorption of enflurane at room temperature is broad and asymmetrical. As illustrated in Figure 4 (see the inset), the matrix spectrum shows at the high-frequency side of the main νC4H12 absorption the spectroscopic features that may arise from the presence of other species than enflurane monomers. This will be discussed in the next section.

3.3. Optimized Geometry and NBO Analysis of the Enflurane Dimer. Some spectroscopic observations such as the influence of the concentration on the infrared spectrum of enflurane and the presence of the additional high frequency absorptions in the argon matrix suggest that some higher associates are formed in solution and in argon. To have a better insight into the vibrational properties of enflurane, we have in a first stage investigated the theoretical properties of the enflurane dimer.

The optimized structure of the most stable enflurane dimer is displayed in Figure 5. This figure shows that the dimer is formed by the A_1 and A_2 subunits, which have both the t,T,g conformation, similar to that of A. These two subunits are held together by two CH···F hydrogen bonds, the CH group of the CHFCl group acting as proton donor and one of the F atoms of the CHF_2 group acting as proton acceptor. As shown by the large H22···O3 and H5···O13 distances equal to 3.458 and 3.045 Å, respectively, there is negligible interaction between the C−H bonds and the O atoms. This may be accounted for by the low basicity of the O atom, on the one hand, and the good proton donor ability of the C−H bond in the CHFCl group, on the other hand. No experimental or theoretical data are available for the proton affinity (PA) of the oxygen atom of enflurane. Its PA must not markedly differ from the PA of $CHF_2-O-CHF_2$ (153 kcal mol^{-1}) calculated at the B3LYP/6-311++G(d,p) level,[11] whereas the latter is much lower than the PA of CH_3-O-CH_3 (191 kcal mol^{-1}).[13] Our results for enflurane indicate that the CHFCl group is a better proton donor than the CHF_2 group. This may also be anticipated from the fact that the CH···O hydrogen bonds are somewhat stronger in the $CH_2Cl_2\cdots H_2O$ complexes than in the $CH_2F_2\cdots H_2O$ complexes,[14] suggesting a larger acidity of the C−H bond in CH_2Cl_2. The deprotonation enthalpy of the CH_2Cl_2 molecule is indeed equal to 374 kcal mol^{-1} and is lower than the deprotonation enthalpy of CH_2F_2 equal to 387 kcal mol^{-1}. Interestingly, recent theoretical calculations have shown that dimethyl ether can be involved in the formation of a cyclic dimer with two molecules being held together by CH···O hydrogen bonds.[15] The interaction energy between the two dimethyl ether molecules calculated at the MP2/6-311G(d) level is equal to −2 kcal mol^{-1}. In the present case, the CP-corrected interaction energy between two enflurane molecules in the dimer, calculated at the MP2/6-311G(d) level of theory, is also equal to about −2 kcal mol^{-1}.

TABLE 6: Relevant B3LYP/6-31G(d) Optimized Geometric Parameters in the A Conformer and in the Two Subunits of the $A_1\cdots A_2$ Dimer (Distances in Å, Angles in deg)

intramolecular parameters	A	A_1	A_2
C1−H5	1.0909	1.0895	1.0884 (C16H22)
C4−H12	1.0912	1.0910	1.0906 (C14H17)
C2−O3	1.373	1.377	1.378 (C15O13)
O3−C4	1.399	1.391	1.393 (O13C14)
C1−F6	1.357	1.358	1.358 (C16F23)
C4−F10	1.348	1.360	1.352 (C14F18)
C4−F11	1.342	1.339	1.345 (C14F19)

intermolecular parameters	$A_1\cdots A_2$
H5···F18	2.348
H22···F10	2.330
H5···O13	3.045
H22···O3	3.458
C1−H5···F18	173.1
C16−H22···F10	134.5

For most of the bonds, the changes induced by the formation of the $A_1\cdots A_2$ dimer of enflurane are rather small. The C1−C2, C2−F8, C2−F9, and C−Cl distances do not differ by more than 0.003 Å in the monomer and in the dimer. The largest geometric changes induced by the interaction between two molecules are reported in Table 6, indicating also relevant intermolecular distances and angles.

The results clearly demonstrate that the enflurane dimer is slightly asymmetrical. The H5···F18 and H22···F10 intermolecular distances are equal to 2.348 and 2.330 Å, respectively, while the two CH···F intermolecular angles are markedly different, taking values of 173.1° and 134.5°, respectively. The largest changes in the distances are predicted for the CHFF and CHFCl groups involved in the interaction. Interestingly, dimer formation results in a contraction of the C−H bond involved in the formation of the intermolecular C−H···F bond. This contraction amounts to 0.0014 and 0.0025 Å for the A_1 and A_2 subunits, respectively. The external C−H bonds undergo very small changes, being shortened by 0.0002 and 0.0006 Å. From these contractions, blue shifts of the corresponding νC−H vibrations can be anticipated. This will be discussed in the next section. A small elongation of the C4−F10 (C14−F18) bonds and a small shortening of the C1−F6 (C16−F23) bonds are also worth mentioning.

The present results can be compared with the reported data dealing with the self-association of molecules through the C−H bonds. One of the stable structures of the CH_3F homodimer is the centrosymmetric one, with the two molecules being held together by C−H···F−C hydrogen bonds. As revealed by calculations at the MP2/6-31+G(d,p) level, the C−H bond is shortened by 0.0014 Å, and the C−F bond is elongated by 0.0069 Å.[16] Ab initio or cryospectroscopic studies performed for the $F_3CH\cdots CD_2F_2$ or $F_3CH\cdots FCD_3$ systems indicate similar trends, a contraction of the C−H bond and an elongation of the C−F bond(s).[17]

Table 7 lists NBO data (atomic charges, occupations of antibonding orbitals, hyperconjugation energies, and hybridization of the carbon bonded to the hydrogen) that are pertinent for the discussion. Data for the A monomer, useful for the comparison, are also included in this table.

TABLE 7: Relevant NBO Data for the $A_1\cdots A_2$ Dimer

hyperconjugation energies[a] (kcal mol^{-1})			
	A_1		A_2
nO3(1) → σ*(C4−H12)	3.7	nO13(1) → σ*(C14−H17)	3.8
nO3(2) → σ*(C2−F8)	14.6	nO13(2) → σ*(C15−F21)	14.1
nO3(2) → σ*(C2−F9)	13.3	nO13(2) → σ*(C15−F20)	13.1
nO3(2) → σ*(C4−F10)	16.0	nO13(2) → σ*(C14−F18)	13.9
nO3(2) → σ*(C4−F11)	4.7	nO13(2) → σ*(C14−F19)	6.5
nF10 → σ*(C16−H22)[a]	1.7	nF18 → σ*(C1−H5)[b]	2.3

NBO charges (*e*)			
atom	A	A_1	A_2
C1	0.129	0.128	0.124 (C16)
H5	0.249	0.253	0.255 (H22)
C4	0.861	0.856	0.856 (C14)
H12	0.183	0.187	0.188 (H17)
F10	−0.363	−0.374	−0.363 (F18)
F11	−0.356	−0.348	−0.357 (F19)
Cl7	−0.031	−0.036	−0.032 (Cl24)

occupation of antibonding σ* orbital (*e*)			
bond	A	A_1	A_2
C1−H5	0.033	0.037	0.036 (C16−H22)
C4−H12	0.045	0.045	0.044 (C14−H17)
C2−O3	0.087	0.090	0.090 (C15−O13)
O3−C4	0.087	0.083	0.083 (O13−C14)
C4−F10	0.091	0.100	0.090 (C14−F18)
C4−F11	0.081	0.076	0.085 (C14−F19)

% s − character			
bond	A	A_1	A_2
C1−H5	29.23	29.99	29.88 (C16H22)
C4−H12	32.75	32.76	32.89 (C14H17)

[a] nOX(1) is the first lone-pair orbital ($sp^{1.5}$ hybridization) on the oxygen atom X, nOX(2) is the second lone-pair orbital (p_z) on the oxygen atom (X = O3 or O13). [b] Sum of the hyperconjugation energies from the three F lone pairs to the corresponding σ*(C−H) orbitals.

Formation of the dimer does not result in spectacular changes of the hyperconjugative energies in each subunit. The largest change is predicted for the nO3(2) → σ*(C4−F10) hyperconjugation, which is larger by 2.5 kcal mol^{-1} in the A_1 subunit than in the A monomer. This effect is accompanied by an elongation of the C4−F10 bond (by 0.012 Å) along with an increase in occupation of the σ*(C4−F10) orbital. A reverse effect is predicted for the C4−F11 bond that is slightly contracted with respect to the monomer.

Perusal of the data shows that there is a global charge transfer of 0.0025 *e* from the A_1 to the A_2 subunit one. This also indicates the nonequivalence of the two enflurane molecules in the dimer. In the CH···F intermolecular bond, the total hyperconjugative energy from the three F lone pair orbitals to the σ*(C−H) orbital is small, of the order of magnitude of 2 kcal mol^{-1}, in both subunits. The formation of the CH···FC intermolecular bond results in a small increase of the positive charge on the bonding proton, similar to conventional hydrogen bonds along with a small increase of the negative charge on the F atom involved in the interaction. As shown in Table 7, the asymmetrical charge distribution in the dimer is demonstrated by the charge on the external Cl atoms, which is equal to −0.036 *e* in the A_1 subunit and to −0.032 *e* in the A_2 one (in the A conformer is equal to −0.031 *e*). This clearly indicates that there is a charge transfer in the remote part of the complex for the A_1 subunit but not for the A_2 one.

In the present case, dimer formation results in a small increase in the occupation of the σ*(C1−H5) (C16−H12) orbitals, by 0.004 and 0.003 *e*, respectively. The C−H bond shortening may be due to an increase in the s-character, which is ca. 0.7% larger with respect to the monomer. This is in full agreement with the theory of Alabugin et al.,[18] who have shown that the C−H bond length is governed by a subtle balance between hyperconjugation and rehybridization. This is also in accordance with previous results on complexes between methyl halides and hydrogen peroxide, where a dual expression between the C−H bond length, on the one hand, and the σ*(C−H) occupation and the hybridization of the C atom bonded to H, on the other hand, has been deduced.[19]

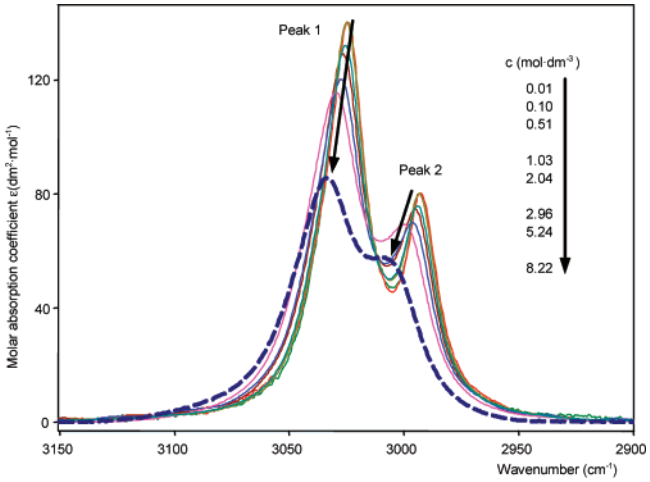

Figure 6. Influence of the concentration on the ν(CH) bands of enflurane. The spectrum of neat enflurane is marked by a dashed line. Trends of the spectral changes with increasing concentration of enflurane are indicated by arrows.

Similar results have been recently obtained for the $F_3CH\cdots FCD_3$ systems. The interaction between the molecules results in a small contraction of the C−H bond, an increase of the σ*(C−H) occupation, and an increase of the s-character of the C−H bond.[17b] It must be mentioned that in strong CH···C$^-$ hydrogen bonds involving homoconjugated carbanions or in strong CH···X$^-$ hydrogen bonds between halogenomethanes and halide ions, the occupation of the σ*(C−H) orbital has a decisive influence on the C−H bond length.[20]

3.4. Infrared Spectra of the $A_1\cdots A_2$ Dimer. In this section, we discuss the experimental infrared spectra observed in solution and in argon matrix. The assignment of the vibrational modes of the enflurane dimer, calculated at the B3LYP/6-31G(d) level, is discussed as well. It may be mentioned that due to the narrowing of the absorption bands, the results in noble gases matrices[21] or in liquefied noble gases[22] are particularly interesting for weakly interacting systems, where the shifts induced by molecular interactions are small.

The infrared spectra (3150−2900 cm^{-1}) recorded at different enflurane concentrations in carbon tetrachloride are reproduced in Figure 6. As illustrated in Figure 7, the absorptions observed at 3024 and 2992 cm^{-1} in dilute carbon tetrachloride are progressively shifted to higher wavenumbers on increasing the concentration, and are observed at 3034 and 3005 cm^{-1} in neat enflurane. The blue shifts of the νC−H vibrations are equal to 10 and 13 cm^{-1}, respectively. An increase of the CH stretching frequency is accompanied by a marked decrease of the infrared intensity, which characterizes the blue-shifting hydrogen bonds.[23] In contrast, intermolecular interactions involving polar OH or NH groups usually cause a red frequency shift of the corresponding stretching vibrations, being accompanied by an increase of the infrared intensity.

Very few studies on the influence of the concentrations on the frequencies or intensities of blue-shifted bands are available

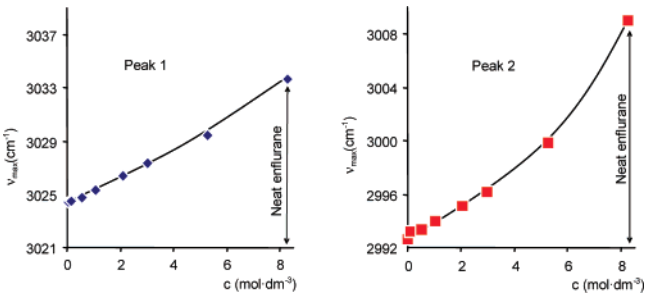

Figure 7. The νCH frequency (cm^{-1}) as a function of the concentration of enflurane (mol dm^{-3}) in carbon tetrachloride.

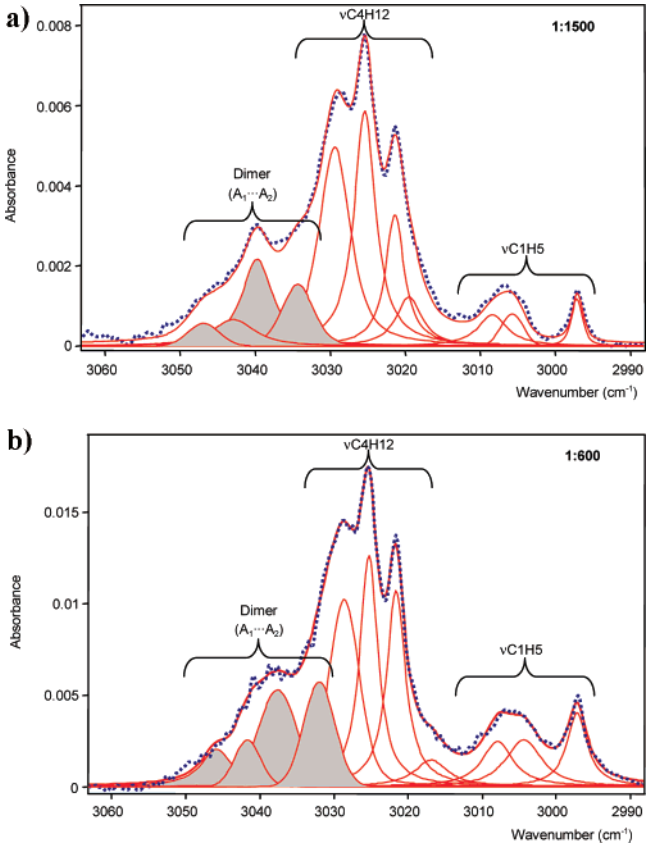

Figure 8. Infrared spectrum (3060−2990 cm^{-1}) of enflurane in argon at two different matrix ratios: (a) 1:1500 and (b) 1:600. Bands assigned to the dimer are indicated by the shadowed area.

in the literature. In the Raman spectrum of 4-methoxybenzaldehyde, a small difference of the aldehydic νCH mode has been observed in dilute solution in carbon tetrachloride and in the neat compound.[24] It has also been observed that the frequencies of the νCH stretching modes of 1,4-dioxane in water solution increase and the infrared intensities of the modes systematically decrease with increasing concentration of water.[25] This difference has been accounted for by a strong polarization of the water molecules and by the formation of larger hydration clusters formed cooperatively. In the present case, increasing the concentration of enflurane in carbon tetrachloride results in an increase of the polarity of the medium. The calculated dipole moments of the A monomer and the $A_1\cdots A_2$ dimer are indeed equal to 0.76 and 1.40 D, respectively. However, due to the broadness of the observed bands, no splitting for the CH···F contacts and bulk solvents effects could be observed as in the case of the interaction between chloroform and ethylacetate.[26] Interestingly, a recent theoretical investigation of Scheiner et al.[27] has shown that there is a progressively diminished blue shift of the C−H stretching frequency in bonded C−H···O groups as the solvent becomes more polar.

Other vibrational modes of enflurane show small concentration dependence. In very dilute solution, absorptions are observed at 1150, 1132, and 1108 cm^{-1} (Table 5). In neat enflurane, the band at 1150 cm^{-1} disappears and overlaps with the broad absorption at ca. 1130 cm^{-1}. This band is assigned to the Q9 mode with a predominant νC14F18 or νC4F11 contribution. Further, the absorption at 1108 cm^{-1} is shifted to lower frequencies at ca. 1100 cm^{-1}. Also, the band at 1267 cm^{-1} in dilute solution, which is generated predominantly by the βH5CC vibration, shifts to 1269 cm^{-1} in neat enflurane.

Table 8 contains the spectral parameters relative to the $A_1\cdots A_2$ dimer, the absorptions observed in argon matrix, the calculated frequencies, infrared intensities, and the assignment of the vibrational modes including the PED. This table also indicates the experimental and calculated frequency shifts with respect to the monomer. In the spectrum in argon matrix illustrated in Figure 4, the high-frequency bands attributed to dimer are shadowed.

Figure 8 shows the spectra taken with two different matrix ratios equal to 1:1500 and 1:600. For both of the spectra, deconvolution (without any constraints) of the broad absorptions between 3030 and 3050 cm^{-1} has led to four components corresponding to the four C−H stretching vibrations in dimer, which is supported by the DFT calculations. As follows from comparison shown in Figure 8a and b, a higher intensity of these components has been obtained for a bigger concentration of enflurane in argon matrix. Annealing the matrix up to 30 K did not cause marked changes of the infrared intensities of the dimer bands.

Our calculations indicate that the νCH vibrations of the two subunits in the dimer are not coupled. The calculated frequency shifts of the stretching vibrations of the C16−H22 and C1−H5 groups involved in the CH···F hydrogen bond are 38 and 30 cm^{-1}, respectively. This is in good agreement with the shifts of 39 and 35 cm^{-1} observed in argon matrix. The calculations also predict a spectacular decrease of the infrared intensity from 8 km mol^{-1} in the A monomer to 2 or 3 km mol^{-1} in the dimer. This is also consistent with the experimental spectra showing that the bands at 3047 and 3043 cm^{-1} are very weak. It should be mentioned that the calculations also predict a small blue shift of 11 and 4 cm^{-1} for the two external C−H bonds, which is consistent with the small contraction of these bonds. Somewhat larger experimental shifts, that is, 15 and 9 cm^{-1}, may be due to imprecision in the deconvolution of the spectra, as the bands of the monomers strongly overlap with the shifted absorptions attributed to the dimer.

The formation of the dimer results in perturbations of other vibrational modes. It may be mentioned that the two components of the mode Q7 can be observed at 1271 and 1268 cm^{-1} in argon matrix; they are red-shifted by 5 and 2 cm^{-1} from the monomer. Also, the band culminating at 1108 cm^{-1} in solution splits into two components, at 1102 and 1097 cm^{-1} in argon. The largest shifts are observed for vibrations involving the C−F bonds. The mode observed at 1150 cm^{-1} in argon matrix, which is attributed predominantly to the νC14F18 vibration, is red-shifted by 13 cm^{-1}. Moreover, the mode Q12 observed at 1097 cm^{-1} and assigned to the νC4F10 vibration is red-shifted by 14 cm^{-1}. This is in relative good agreement with the calculations predicting frequency lowering of 18 and 22 cm^{-1}, respectively, for these two modes. These shifts may be related to the elongations of the C4−F10 and C14−F18 bonds previously discussed.

TABLE 8: Experimental Frequencies in Argon, B3LYP/6-31G(d) Calculated Frequencies (cm^{-1}), and Infrared Intensities (km mol^{-1}, in Parentheses) in the $A_1\cdots A_2$ Dimer, Assignment of the Vibrational Modes, and Frequency Shifts ($\Delta\nu$) Resulting from the Interaction[a]

mode	ν^{exp}	$\Delta\nu^{exp}$	ν^{calc}	$\Delta\nu^{calc}$	assignment and PED
Q2	3047	+39	3189 (3)	+38	νC16H22 (100)
Q2	3043	+35	3181 (2)	+30	νC1H5 (100)
Q1	3040	+15	3166 (24)	+11	νC14H17 (100)
Q1	3034	+9	3161 (29)	+4	νC4H12 (100)
Q5	1364	+5	1417 (32)	+9	γH12CO (43), βH22CC (14)
Q5	1359	0	1404 (40)	−4	βH22CC (34), γH12CO (24)
Q7	1271	+5	1307 (112)	+6	βH5CC (23), ν^{s}C2FF (16)
Q7	1268	+2	1305 (164)	+4	βH22CC (25), ν^{s}C5FF (17)
Q8	1191	−3	1208 (341)	−4	νC2O3 (42), νC15O13 (29)
Q8	1187	−7	1205 (305)	−7	νC15O13 (45), νC2O3 (21)
Q9	1169	+6	1200 (271)	+4	νC4F11 (59); ν^{as}C15FF (10)
Q9	1150	−13	1178 (145)	−18	νC14F18 (44), ν^{as}C15FF (24)
Q10	1138	+3	1160 (213)	+2	ν^{as}C2FF (24), νC14F19 (17)
Q10	n.o.		1159 (377)	+1	νC14F19 (47), ν^{as}C2FF (13)
Q11	1120	−7	1144 (353)	−8	νC14F18 (26), νC1F6 (19)
Q11	n.o.		1137 (87)	−15	νC1F6 (42), νC16F23 (26)
Q12	1102	−9	1132 (31)	−6	νC16F23 (49), νC1F6 (18)
Q12	1097	−14	1115 (196)	−22	νC4F10 (66), wC4FF (10)
Q13	1071	+13	1089 (376)	+18	νC2O3 (60), νC14O13 (11)
Q13	n.o.		1082 (78)	+11	νC14O13 (62), νC4O3 (12)
Q14	888	+2	898 (7)	+1	ν^{s}C15FF (36), ν^{s}C2FF (15)
Q14	n.o.		895 (1)	−2	ν^{s}C2FF (34), ν^{s}C15FF (15)
Q15			809 (27)	+2	νC16Cl24 (43)
Q15			804 (198)	−3	νC1Cl7 (43)
Q16	750	+4	756 (150)	+2	wC2FF (34), ν^{s}C15FF (13)
Q16	n.o.		752 (1)	−2	wC15FF (44), wC2FF (13)

[a] Abbreviations as in Table 4.

The results collected in Table 8 indicate that there is a relatively good agreement between the frequency shifts observed in argon and the calculated ones. This suggests that the $A_1\cdots A_2$ dimer is the predominating associated species in argon medium. However, the coexistence of higher aggregates in neat enflurane and in concentrated solutions cannot be excluded.

4. Concluding Remarks

The most important findings of this work are the following:

(1) Theoretical studies on enflurane ($CHFCl-CF_2-O-CHF_2$) performed at the B3LYP/6-31G(d) and MP2/6-311G(d) levels of theory show that the four most stable conformers possess a trans configuration of the C−C−O−C skeleton and gauche orientation of the CHF_2 group (with respect to the central C−O bond). These results are in agreement with previously reported data from gas electron diffraction and quantum chemical studies. The present calculations reveal that these conformations are favored by electrostatic interaction between the H atom of the CHF_2 group and the F atoms of the central CF_2 group. Natural Bond Orbital (NBO) analysis shows that hyperconjugation effects from the O lone pairs to the antibonding orbitals of the neighboring C−H and C−F bonds also contribute to the stability of the four conformers.

(2) Experimental infrared spectra of enflurane have been investigated in carbon tetrachloride solution at room temperature and in argon matrix at 12 K. The vibrational frequencies, infrared intensities, and potential energy distributions (PEDs) are calculated for the most stable conformers using the B3LYP/6-31G(d) method. The detailed vibrational assignment of the experimental spectra is reported, for the first time. On the basis of the theoretical results, the four conformers of enflurane are identified in an argon matrix. Studies in CCl_4 solution have revealed the influence of the concentration on the ν(CH) vibrations, which suggests the formation of higher aggregates in solution and in neat enflurane.

(3) Theoretical calculations are carried out on the enflurane dimer. The results show that the dimer is formed between two enflurane conformers having the largest stability. The dimer has an asymmetric cyclic structure, the two enflurane molecules being held together by two nonequivalent C−H···F hydrogen bonds, the C−H bond of the CHFCl group acting as a proton donor, and one of the F atoms of the CHF_2 groups acting as a proton acceptor. The two H···F intermolecular distances are equal to 2.348 and 2.330 Å, while the two CH···F intermolecular angles are markedly different, taking values of 173.1° and 134.5°. NBO analysis has revealed that dimerization leads to a charge transfer of 0.0025 *e* between two subunits, and to changes in occupation of antibonding σ^*(C−H) and σ^*(C−F) orbitals.

(4) According to the theoretical predictions, dimer formation results in a contraction of the C−H bond involved in the formation of intermolecular C−H···F bonding (by 0.0014−0.0025 Å) along with a blue shift of 30−38 cm^{-1} of the corresponding ν(C−H) bands. These data are in good agreement with the blue shifts of 35−39 cm^{-1} observed in an argon matrix.

(5) Studies in CCl_4 solution have demonstrated that an increase of the concentration also results in the blue shifts of the νC−H bands. Moreover, it leads to a marked decrease of the infrared intensities of these bands. These effects are consistent with the theoretical results predicting a spectacular decrease of the infrared intensity of the νC−H bands in the spectra of dimer.

Acknowledgment. This work was supported by the Polish Committee for Scientific Research (Grant KBN 7 1 T09A 134 30) and by a grant from the Wrocław University of Technology. The Poznań Supercomputer and Networking Center and the Wrocław Centre for Networking and Supercomputing are acknowledged for generous computer time.

Note Added after Print Publication. The reference list has been corrected to match the citation numbering within the manuscript version published on the Web October 3, 2007 (ASAP) and in the October 25, 2007 issue (Vol. 111, No. 42, pp 12228−12238); the correct electronic version of the paper was posted on February 13, 2008, and an Addition and Correction appears in the March 6, 2008 issue (Vol. 112, No. 9).

References and Notes

(1) (a) Di Paolo, T.; Sandorfy, C. *Nature* **1974**, *252*, 471. (b) Trudeau, G.; Dumas, J. M.; Dupuis, P.; Guérin, M.; Sandorfy, C. *Top. Curr. Chem.* **1980**, *93*, 91. (c) Franks, N. P.; Lieb, W. R. *Nature* **1994**, *367*, 607 and references therein. (d) Sandorfy, C. *Anesthesiology* **2004**, *101*, 1225. (e) Sandorfy, C. *J. Mol. Struct.* **2004**, *708*, 3. (f) Sandorfy, C. *Collect. Czech. Chem. Commun*. **2005**, *70*, 539.

(2) Polavarapu, P. L.; Zhao, C.; Cholli, A. L.; Vernice, G. G. *J. Phys. Chem. B* **1999**, *103*, 6127.

(3) Polavarapu, P. L.; Cholli, A. L.; Vernice, G. *J. Am. Chem. Soc*. **1992**, *114*, 10953.

(4) (a) Balonga, P. E.; Kowalewski, V. J.; Contraras, R. H. *Spectrochim. Acta, Part A* **1988**, *44*, 819. (b) Pfeiffer, A.; Mack, H.-G.; Oberhammer, H. *J. Am. Chem. Soc.* **1998**, *120*, 6384. (c) Zhao, C.; Polavarapu, P. L.; Grosenik, H.; Schurig, V. *J. Mol. Struct.* **2000**, *550*, 105.

(5) (a) Becke, A. D. *J. Chem. Phys.* **1993**, *98*, 5648. (b) Lee, C.; Yang, W.; Parr, R. G. *Phys. Rev. B* **1988**, *37*, 785.

(6) Nowak, M. J.; Lapinski, L.; Bieńko, D. C.; Michalska, D. *Spectrochim. Acta, Part A* **1997**, *53*, 855.

(7) (a) Reed, A. E.; Curtiss, L. A.; Weinhold, F. *Chem. Rev*. **1988**, *88*, 899. (b) Glendening, E. D.; Reed, A. E.; Carpenter, J. E; Weinhold, F. *NBO 3.1*; Theoretical Chemistry Institute, University of Wisconsin, Madison, WI, 1996.

(8) (a) Boys, S. F.; Bernardi, F. *Mol. Phys.* **1970**, *19*, 553. (b) Simon, S.; Duran, M.; Dannenberg, J. J. *J. Chem. Phys.* **1996**, *105*, 11024. (c) Frisch, M. J.; Trucks, G. W.; Schlegel, H. B.; Scuseria, G. E.; Robb, M. A.; Cheeseman, J. R.; Montgomery, J. A.; Vreven, T.; Kudin, K. N.; Burant, J. C.;. Millam, J. M.; Iyengar, S. S.; Tomasi, J.; Barone, V.; Cossi, M.; Scalmani, G.; Rega, N.; Peterson, G. A.; Nakkatsuji, H.; Hada, M.; Ehara, M.; Toyota, K.; Fukuda, R.; Hasegawa, J.; Ishida, M.; Nakajima, T.; Honda, Y.; Kitao, O.; Nakai, H.; Klene, M.; Li, X.; Knox, J. E.; Hratchian, H. P.; Cross, J. B.; Bakken, V.; Adamo, C.; Jaramillo, J.; Gomperts, R.; Stratman, R. E.; Yazyev, O.; Austin, A. J.; Cammi, R.; Pomelli, C.; Ochterski, J. W.; Ayala, P. Y.; Morokuma, K.; Voth, G. A.; Salvator, P.; Dannenberg, J. J.; Zakrzewski, V. G.; Dapprich, S.; Daniels, A. D.; Strain, M. C.; Farkas, D. K.; Malick, D. K.; Rabuck, A. D.; Raghavachari, K.; Foresman, J. B.; Ortiz, J. V.; Cui, Q.; Baboul, A. G.; Clifford, S.; Ciolowski, B. B.; Stefanov, B. B.; Liu, G.; Liashenko, A.; Piskorz, P.; Komaromi, I.; Martin, R. L.; Fox, D. J.; Keith, T.; Al-Laham, M. A.; Peng, C. Y.; Nanayakkara, A.; Challacombe, M.; Gill, P. M. W.; Johnson, B. G.; Chen, W.; Wong, M. W.; Gonzales, C.; Pople, J. A. *Gaussian 03*, revision D.01; Gaussian, Inc.: Wallingford, CT, 2004.

(9) For leading references, see, for example; (a) Schleyer, P. v. R.; Kos, A. *Tetrahedron* **1983**, *39*, 1141. (b) Reed, A. E.; Schade, C.; Schleyer, P. v. R.; Kamath, P. V.; Chandrasekhar, J. *J. Chem. Soc., Chem. Commun*. **1988**, 67. (c) Salzner, U.; Schleyer, P. v. R. *J. Am. Chem. Soc*. **1993**, *115*, 10231 and references therein. (d) Alabugin, I. V.; Zeidan, T. A. *J. Am. Chem. Soc*. **2002**, *124*, 3175.

(10) (a) Jeffrey, G. A.; Yates, J. H. *J. Am. Chem. Soc*. **1979**, *101*, 820. (b) Durig, J. R.; Lin, J. A.; van der Veken, B. *J. Struct. Chem*. **1993**, *4*, 103. (c) Kuhn, R.; Christen, D.; Mack, H.-G.; Konikowski, D.; Minkwitz, R.; Oberhammer, H. *J. Mol. Struct*. **1996**, *376*, 217. (d) Radice, S.; Toniolo, P.; Avataneo, M.; De Patto, U.; Marchionni, G.; Castiglioni, C.; Tommasini, M.; Zerbi, G. *J. Mol. Struct. (THEOCHEM)* **2004**, *710*, 151.

(11) Nam, P.-C.; Nguyen, M.-T.; Zeegers-Huyskens, Th. *J. Mol. Struct. (THEOCHEM)* **2007**, *821*, 71.

(12) Barnes, A. J. *Molecular Interactions*; John Wiley & Sons: Chichester, New York, 1980; Vol. 1, p 273.

(13) Lias, S. G.; Bartmess, J. E.; Liebman, J. F.; Holmes, J. L.; Levin, R. D.; Maillard, W. G. *J. Phys. Chem. Ref. Data* **1988**, *17* (Suppl. 1), 872.

(14) Kryachko, E. S.; Zeegers-Huyskens, Th. *J. Phys. Chem. A* **2001**, *105*, 2527.

(15) Bleiholder, C.; Werz, D. B.; Köppel, H.; Gleiter, R. *J. Am. Chem. Soc.* **2006**, *128*, 2666.

(16) Kryachko, E. S.; Scheiner, S. *J. Phys. Chem. A* **2004**, *108*, 2527.

(17) (a) Rutkowski, K. S.; Rodziewicz, P.; Melikova, S. M.; Herrebout, W. A.; van der Veken, B. J.; Koll, A. *Chem. Phys*. **2005**, *313*, 225. (b) Rutkowski, K. S.; Rodziewicz, P.; Melikova, S. M.; Koll, A. *ChemPhysChem* **2005**, *6*, 1282.

(18) Alabugin, I. V.; Manoharan, M.; Peabody, S.; Weinhold, F. *J. Am. Chem. Soc.* **2003**, *125*, 5973.

(19) (a) Nguyen, H. M. T.; Nguyen, M. T.; Peeters, J.; Zeegers-Huyskens, Th. *J. Phys. Chem. A* **2004**, *108*, 11101. (b) Nguyen, H. M. T.; Peeters, J.; Zeegers-Huyskens, Th. *J. Mol. Struct.* **2006**, *793*, 16.

(20) (a) Chandra, A. K.; Zeegers-Huyskens, Th. *J. Phys. Chem. A* **2005**, *109*, 12006. (b) Kryachko, E. S.; Zeegers-Huyskens, Th. *J. Phys. Chem. A* **2002**, *106*, 6832.

(21) (a) Matsuura, H.; Yoshida, H.; Hieda, M.; Yamanaka, S.-Y.; Shin, Y. K.; Ohno, K. *J. Am. Chem. Soc*. **2003**, *125*, 13010. (b) Ahokas, J. M.; Vaskonen, K. J.; Kunttu, H. M. *J. Phys. Chem. A* **2006**, *110*, 7816.

(22) (a) Van der Veken, B. J.; Herrebout, W. A.; Szostak, R.; Shchepkin, D. N.; Havlas, Z.; Hobza, P. *J. Am. Chem. Soc*. **2001**, *123*, 12290. (b) Delanoy, S. N.; Herrebout, W. A.; van der Veken, B. J. *J. Am. Chem. Soc*. **2002**, *124*, 7490.

(23) "Blue-shifting" hydrogen bonds have engendered numerous recent studies intended to understand the source of this contrasting behavior. See, for example: (a) Gu, Y.; Kar, T.; Scheiner, S. *J. Am. Chem. Soc*. **1999**, *121*, 9411. (b) Desiraju, G. R. *Acc. Chem. Res.* **2002**, *35*, 565. (c) Hobza, P.; Havlas, Z. *Theor. Chem. Acc*. **2002**, *108*, 325. (d) Masunov, A.; Dannenberg, J. J.; Contreras, R. H. *J. Phys. Chem. A* **2001**, *105*, 4737. (e) Hermansson, K. *J. Phys. Chem. A* **2002**, *106*, 4695. (f) Wetmore, S. D.; Schofield, R.; Smith, D. M.; Radom, L. *J. Phys. Chem. A* **2001**, *105*, 8718. (g) Li, X.; Liu, L.; Schlegel, H. B. *J. Am. Chem. Soc*. **2002**, *124*, 9639. (h) Pejov, L.; Hermansson, K. *J. Chem. Phys*. **2003**, *119*, 313. (i) Alabugin, I. V.; Manoharan, M.; Weinhold, F. F. *J. Am. Chem. Soc*. **2004**, *108*, 4720. (j) Alonso, J. L.; Antolines, S.; Blanco, S.; Lesarri, A.; Lopez, J. C.; Carminati, W. *J. Am. Chem. Soc*. **2004**, *126*, 3244. (k) McDowell, S. A. C.; Buckingham, A. D. *J. Am. Chem. Soc*. **2005**, *127*, 15515 and references therein. (l) Yang, Y.; Zhang, W.; Gao, X. *Int. J. Quantum Chem*. **2006**, *106*, 1199.

(24) (a) Karger, N.; Amorin da Costa, A. H.; Ribeiro-Claro, P. J. A. *J. Phys. Chem. A* **1999**, *103*, 8672. (b) Marques, M. P. M.; Amorin da Costa, A. M.; Ribeiro-Claro, P. J. A. *J. Phys. Chem. A* **2001**, *105*, 5292.

(25) Mizuno, K.; Imafiji, S.; Fujiwara, T.; Ohta, T.; Tamiya, Y. *J. Phys. Chem. B* **2003**, *107*, 3972.

(26) Ribeiro-Claro, P. J. A.; Vaz, P. D. *Chem. Phys. Lett*. **2004**, *390*, 358.

(27) Scheiner, S.; Kar, T. *J. Phys. Chem. B* **2005**, *109*, 3681.